Unified Origin for the 3D Magnetism and Superconductivity in Na_xCoO_2

Kazuhiko Kuroki,[1] Shuhei Ohkubo,[1,*] Takumi Nojima,[1,†] Ryotaro Arita,[2] Seiichiro Onari,[3] and Yukio Tanaka[3]

[1]*Department of Applied Physics and Chemistry, The University of Electro-Communications, Chofu, Tokyo 182-8585, Japan*

[2]*RIKEN, 2-1 Hirosawa, Wako, Saitama 351-0198, Japan*

[3]*Department of Applied Physics, Nagoya University, Nagoya 464-8603, Japan*

(Received 18 October 2006; published 27 March 2007)

We analyze the origin of the three-dimensional (3D) magnetism observed in nonhydrated Na-rich Na_xCoO_2 within an itinerant spin picture using a 3D Hubbard model. The origin is identified as the 3D nesting between the inner and outer portions of the Fermi surface, which arise due to the local minimum structure of the a_{1g} band at the Γ-A line. The calculated spin wave dispersion strikingly resembles the neutron scattering result. We argue that this 3D magnetism and the spin fluctuations responsible for superconductivity in the hydrated systems share essentially the same origin.

DOI: 10.1103/PhysRevLett.98.136401 PACS numbers: 74.70.−b, 71.10.−w, 75.30.Ds

The discovery of superconductivity (SC) in $Na_xCoO_2 \cdot y H_2O$ has attracted much attention [1]. Although the experiments are still somewhat controversial, we briefly summarize the present understanding. (i) Up to now, all of the angle resolved photoemission (ARPES) measurements [2–5] show the absence of the e_g' hole pockets predicted in the first principles calculation [6]. Thus, the remaining a_{1g} seems to be the relevant band. (ii) In the bilayer hydrated (BLH) SC samples, there is an enhancement in $(T_1T)^{-1}$ at low temperatures at the Co site [7–11] and at the O site [9,12] (T_1^{-1} is the spin-lattice relaxation rate), indicating the presence of spin fluctuations (SF) located away from the Brillouin zone (BZ) edge [9,12], while such an enhancement is not seen in non-SC monolayer hydrated and nonhydrated Na-poor samples. On the other hand, the Knight shift stays nearly constant at low temperatures in the SC samples [9,12,13], which means that the SF is not purely ferromagnetic. The bottom line is that SF that is neither purely ferromagnetic nor antiferromagnetic is strongly related to SC. (iii) Unconventional SC gap is suggested from the absence of the coherence peak in T_1^{-1} as well as the power law decay below T_c [7,8,14,15]. Several experiments suggest spin singlet pairing [14,16], and, moreover, the effect of the impurities on T_c is found to be small [17,18], suggesting an s-wavelike gap.

In a previous paper, as a solution for understanding these experimental results, we have proposed a mechanism for an unconventional s-wave pairing, in which the local minimum structure (LMS) of the a_{1g} band at the Γ point plays an important role [19]. For appropriate band fillings, LMS results in disconnected inner and outer Fermi surfaces (FS), whose partial nesting induces SF at wave vectors that bridge the two FS (see Fig. 4, left panel). This incommensurate SF can give rise to an "extended s-wave" pairing in which the gap changes sign between the two FS but not within each FS. A recent multiorbital analysis also shows that such a pairing can occur when the inner and outer a_{1g} FS are present [20].

The purpose of this paper is to investigate the relation between this SC and the 3D spin-density-wave(SDW)-like, metallic magnetism observed in the nonhydrated Na-rich systems [21–24], whose magnetic structure has been revealed by neutron scattering experiments to have in-plane ferromagnetic and out-of-plane antiferromagnetic character [25,26]. Neutron scattering experiments have further obtained the spin wave dispersion of this 3D magnetism. Analysis of this dispersion based on the localized spin picture has shown that the out-of-plane antiferromagnetic coupling is of the order of the in-plane ferromagnetic coupling [25–27], despite the strong 2D nature of the material. Moreover, the Curie-Weiss (CW) temperature is expected to be positive from the evaluated coupling constants [25], while it is actually negative [13,21–24,28,29]. A theory based on a spin-orbital polaron picture has been proposed for this puzzle [30].

In the present study, since the system remains metallic in the magnetically ordered state, we take an itinerant spin viewpoint. From the consistency between the experiments and the calculated results, we propose that the origin of the 3D magnetism is essentially the same with the SF responsible for SC: The nesting between inner and outer portions of the FS that arises due to the local minimum of the a_{1g} band [31].

There exist two CoO_2 layers within a unit cell due to the alternation of the oxygen arrangement, but neither the effective hopping integrals nor the on-site energy alter along the c axis, so the BZ folding in the c direction occurs without inducing a gap in the band. Thus, in a 3D effective theory in which O and Na site degrees of freedom are integrated out, the unit cell contains only one layer, which results in an unfolded BZ shown in the upper right in Fig. 1. Taking into account only the a_{1g} band, we consider a single band Hubbard model $H = \sum_{i,j}\sum_\sigma t_{ij} c_{i\sigma}^\dagger c_{j\sigma} + U\sum_i n_{i\uparrow} n_{i\downarrow}$, on a 3D triangular lattice, where the 1st, 2nd, and 3rd neighbor in-plane hopping integrals t_1, t_2, t_3, and the out-of-plane nearest neighbor hopping t_z (Fig. 1, upper left) are chosen so as to roughly reproduce the a_{1g} portions of the

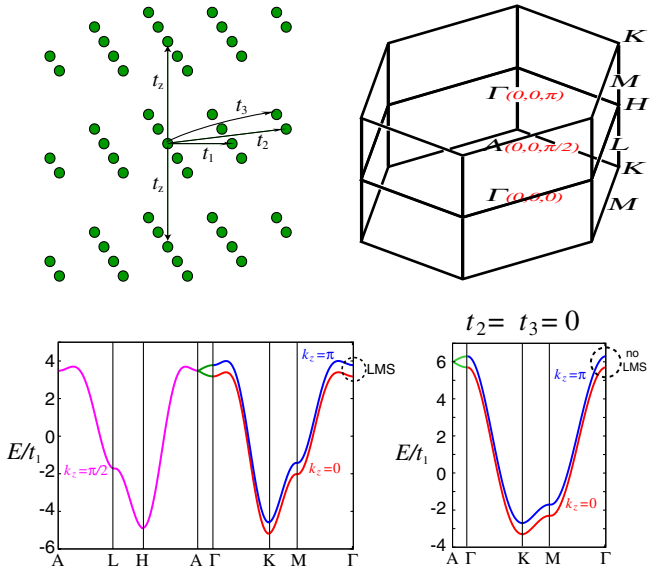

FIG. 1 (color online). Upper left: The 3D model in the present study. Upper right: The Brillouin zone. The wave numbers in the parentheses are those in the unfolded BZ scheme. Lower left: The band structure of the present model with $t_2 = -0.35$, $t_3 = -0.07$, $t_z = -0.15$, and $U = 0$. Lower right: The band for $t_2 = t_3 = 0$, $t_z = -0.15$. $k_z = 0$, $\pi/2$, π are k_z in the unfolded BZ scheme.

band obtained in the first principles calculation [6]. Throughout this Letter, we take $t_2 = -0.35$, $t_3 = -0.07$, and $t_z = -0.15$ (unless otherwise noted) in units of $t_1 = 1$, which corresponds to about (or slightly less than) 0.1 eV according to ARPES measurements [4]. The band (with $U = 0$) for this choice of parameter values is shown in the lower left in Fig. 1. The band filling is $n =$ number of electrons/site, and it is related to the actual Na content x by $n - 1 = x$ (provided that the e_g' bands are fully occupied). We calculate the spin susceptibility using the fluctuation exchange (FLEX) approximation [32] as $\chi_s(q) = \chi_{\rm irr}(q)/[1 - U\chi_{\rm irr}(q)]$, where $q = (\boldsymbol{q}, i\omega_n)$. Here the irreducible susceptibility is $\chi_{\rm irr}(q) = -\frac{1}{N}\sum_k G(k+q)G(k)$ (N: number of k-point meshes), where G is the renormalized Green's function self-consistently obtained from the Dyson's equation, in which the self-energy is calculated using G and $\chi_{\rm irr}$. We take up to $N = 64 \times 64 \times 64$ k-point meshes and up to 16 384 Matsubara frequencies.

In order to analyze the magnetically ordered state with a wave vector $\boldsymbol{Q}$ at which the FLEX spin susceptibility is maximized, we consider a mean field Hamiltonian

$$H = \sum_{\sigma=\uparrow,\downarrow}\sum_{\boldsymbol{k}}\sum_{m=0,1}\Big[\varepsilon(\boldsymbol{k}+m\boldsymbol{Q})c^\dagger_{\boldsymbol{k}+m\boldsymbol{Q},\sigma}c_{\boldsymbol{k}+m\boldsymbol{Q},\sigma} + U\sum_{l=0,1}\langle n_{m\boldsymbol{Q},-\sigma}\rangle c^\dagger_{\boldsymbol{k}+(m+l)\boldsymbol{Q},\sigma}c_{\boldsymbol{k}+m\boldsymbol{Q},\sigma}\Big] = \sum_{\sigma=\uparrow,\downarrow}\sum_{\boldsymbol{k}}\sum_{\alpha=1,2}E_{\alpha,\sigma}(\boldsymbol{k})\gamma^\dagger_{\boldsymbol{k},\sigma,\alpha}\gamma_{\boldsymbol{k},\sigma,\alpha},$$

where $\varepsilon(\boldsymbol{k})$ is the bare band dispersion, $c_{\boldsymbol{k}+m\boldsymbol{Q},\sigma} = \sum_{\alpha=1,2}u_{\alpha,\sigma,m}(\boldsymbol{k})\gamma_{\boldsymbol{k},\sigma,\alpha}$ is a unitary transformation that diagonalizes the Hamiltonian to obtain the two bands $E_{1\sigma}$ and $E_{2\sigma}$, and $\langle n_{\boldsymbol{Q},\sigma}\rangle$ is self-consistently determined in the usual procedure. We then calculate the irreducible susceptibility matrix by

$$[\chi_0^{\sigma\sigma'}(\boldsymbol{k},\omega)]_{ij} = \frac{1}{N}\sum_{\boldsymbol{p}}\sum_{m,n,\alpha,\alpha'}u_{\alpha,\sigma,m+i}(\boldsymbol{p}+\boldsymbol{k})u_{\alpha,\sigma,m+n+j}(\boldsymbol{p}+\boldsymbol{k})u_{\alpha',\sigma',m+n}(\boldsymbol{p})u_{\alpha',\sigma',m}(\boldsymbol{p})\frac{f(E_{\alpha',\sigma'}(\boldsymbol{p})) - f(E_{\alpha,\sigma}(\boldsymbol{p}+\boldsymbol{k}))}{E_{\alpha,\sigma}(\boldsymbol{k}+\boldsymbol{p}) - E_{\alpha',\sigma'}(\boldsymbol{p}) + \omega + i\epsilon},$$

where $f(E)$ is the Fermi distribution function. The spin wave dispersion can be determined by the condition that the real part of the eigenvalue of the matrix $1 - U\chi_0^{\uparrow\downarrow}(\boldsymbol{q},\omega)$ equals zero. We take up to $N = 192 \times 192 \times 96$ k-point meshes here.

We first show in Fig. 2 the evolution of the 3D FS (with $U = 0$) as the band filling is increased. Here the vertical cross section of the FS is given in the unfolded BZ. The FS is a 2D cylinder for small band filling, that is, for low Na content. As the band filling is increased, an inner FS appears around the Γ point. As in the purely 2D ($\sim$ BLH) case (see Fig. 4 or Ref. [19]), this FS is disconnected from the outer 2D cylindrical FS, but the inner FS is 3D in the nonhydrated case [33]. For larger band fillings, the two FS become connected (around $n = 1.73$), and then finally for higher band fillings it becomes a single 3D FS. The appearance of the 3D FS despite the small t_z is a consequence of LMS of the band along the Γ-A line. In fact, if we take a band (lower right in Fig. 1) that does not have LMS, i.e., for $t_2 = t_3 = 0$ but with the same t_z ($= -0.15$), the FS remains 2D (unless the band filling becomes very close to 2) as shown in Fig. 2 ($n = 1.82$). The 3D evolution of the FS is consistent with the ARPES observations, where the in-plane k_F barely decreases with the increase of the Na content for $x > 0.6$ [3,34]. In fact, the decrease of the FS diameter between $n = 1.60$ and 1.82 for $t_2 = -0.35$, $t_3 = -0.07$ is very small compared to the case of $t_2 = t_3 = 0$ (see the difference in Fig. 2 for $n = 1.82$; although not shown, the FS is almost identical for $n = 1.60$).

In the inset of the upper left in Fig. 3, FLEX results of $\chi_s^{-1}(\boldsymbol{q} = 0, i\omega_n = 0)$ are plotted as functions of T for $U = 6$ and $n = 1.82$ or $n = 1.7$. The CW behavior at high temperatures with a negative CW temperature is consistent with the experiments [9,13,21–24,28,29]. In the upper left in Fig. 3, $T_{\rm SDW}$, defined as the temperature where the maximum value of $U\chi_{\rm irr}$ reaches $\simeq 1$, is plotted as a function of the band filling. $T_{\rm SDW}$ exists only in the regime $1.75 < n < 1.9$, which is consistent with the fact that the magnetic ordering is not observed experimentally for $x < 0.75$ [9,23]. The maximum $T_{\rm SDW}$ corresponds to about 20 K, in agreement with the experiments [21,22,24].

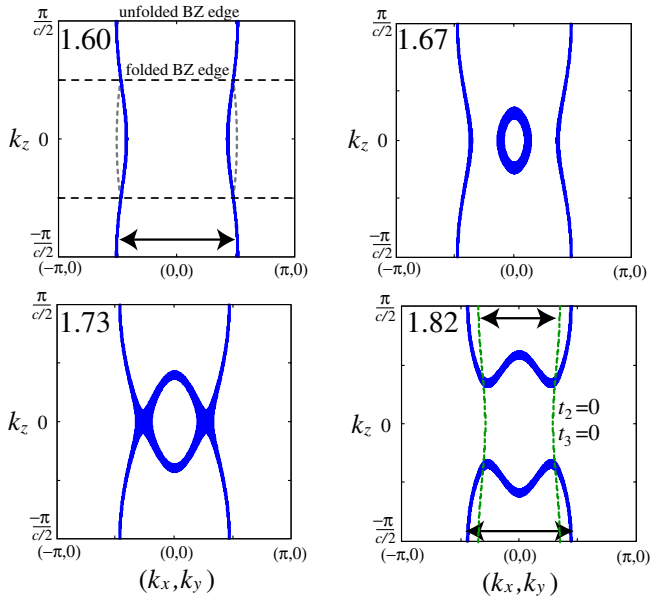

FIG. 2 (color online). The vertical cross section ($k_y = 0$) of the FS for various n (upper left corner) with $U = 0$. Here we use the unfolded BZ scheme, but for $n = 1.60$ we also show the FS in the usual folded BZ scheme by dashed lines. The unfolded BZ edge in the k_z direction is denoted as "$\frac{\pi}{c/2}$" to stress that the unit cell is halved in the c direction. The finite thickness is due to a finite range of energy ($E_F \pm 0.03t_1$) taken in obtaining the FS. The thickness thus represents the density of states or the effective mass. For $n = 1.82$, the FS for $t_2 = t_3 = 0$ (dashed line) is shown for comparison. The arrows represent the diameter of the FS.

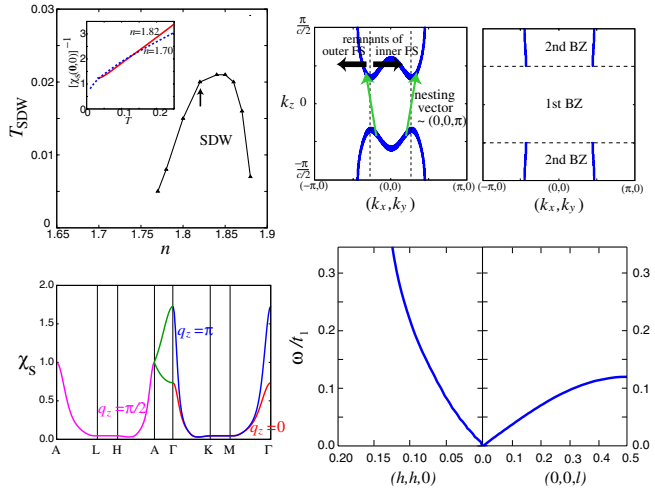

FIG. 3 (color online). Upper left: The band filling dependence of T_{SDW} obtained by FLEX. The inset shows the T dependence of $\chi_s(\mathbf{0}, 0)^{-1}$ for $n = 1.82$ and $n = 1.7$. Upper left: The nesting vector of the FS for $n = 1.82$ (left) and the FS in the ordered state ($T = 0.015$) obtained by the mean field calculation (right) are shown. We use the extended zone scheme in the ordered state, and the regions $0 < |k_z| < \frac{\pi/2}{c/2}$ and $\frac{\pi/2}{c/2} < |k_z| < \frac{\pi}{c/2}$ are the 1st and the 2nd BZ, respectively. Lower left: The FLEX $\chi_s(\boldsymbol{q}, 0)$ for $n = 1.82$, $U = 6$, and $T = 0.05$. Lower right: The calculated in-plane (left) and out-of-plane (right) spin wave dispersion for $n = 1.82$, $U = 4$, and $T = 0.015$. Here the wave vectors are presented in units of the reciprocal lattice primitive vector in the usual *folded* BZ for clear comparison with Fig. 4 of Ref. [25].

Around $n \sim 1.8$, the ordering occurs with $\boldsymbol{Q} = (0, 0, \pi)$, as shown in the lower left in Fig. 3 for $n = 1.82$, which corresponds to in-plane ferromagnetic, out-of-plane antiferromagnetic spin structure, as found experimentally [25,26]. The origin of this spin correlation can be found in the shape of the 3D FS. Namely, the FS at $n \sim 1.8$ is partially nested with a nesting vector close to $(0, 0, \pi)$, as can be seen in Fig. 3 (upper right). In fact, this nesting occurs between portions of the FS that can be considered as remnants of the inner and outer FS, which are disconnected for lower band fillings [35]. On the other hand, as the band filling comes close to $n = 1.9$ ($x = 0.9$), the FS becomes too small for $(0, 0, \pi)$ nesting, and the ordering wave number becomes incommensurate in the c direction, which is also consistent with the finding in Ref. [22].

We now move on to the mean field results in the SDW ordered state. We focus on $n = 1.82$ and take U smaller than $U = 6$ adopted in FLEX since the mean field approach tends to overestimate the tendency toward ordering. In fact, taking $U = 4$ gives a self-consistently determined $\langle n_{Q\uparrow} \rangle$ value of 0.075 at low T, corresponding to a magnetic moment of $0.15\mu_B$ per site (Co atom), in rough agreement with a μSR estimation $0.18\mu_B$ [22]. In Fig. 3 (upper right), we show the calculation result of the FS in the ordered state. The portions of the FS around $k_z = \pm\pi/2$ disappear, but other portions remain to result in a FS with a strong 2D character. This is consistent with the fact that the system remains metallic in the magnetically ordered state [21]. Note also that the disappearing portions of the FS are thick; i.e., they have heavy mass, which is consistent with what has been suggested in Ref. [21] from the enhancement of

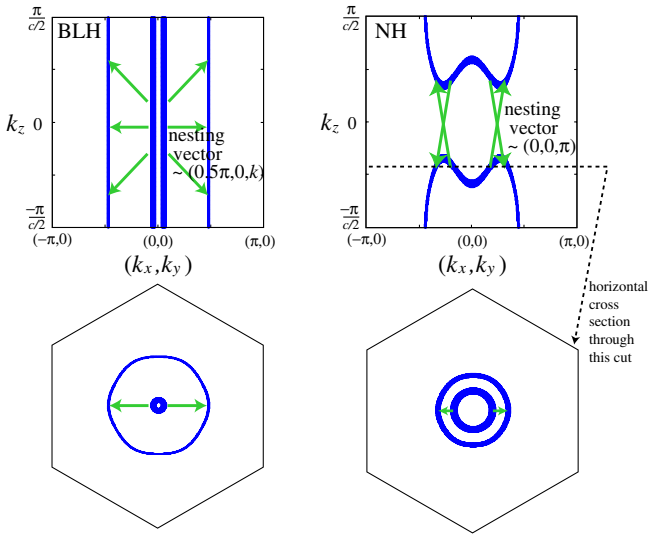

FIG. 4 (color online). The FS nesting relevant for SC (left) and the 3D magnetism (right).

the mobility in the magnetically ordered state. We believe further investigation on the transport properties from the present viewpoint of the FS topology serves as an interesting future study.

In the lower right in Fig. 3, we show the calculated spin wave dispersion. The overall feature as well as the in-plane to out-of-plane ratio $\omega(0.1, 0.1, 0)/\omega(0, 0, 0.5) \sim 2.1$ strikingly resembles the neutron scattering result of Ref. [25] for $x = 0.82$. The energy scale [$\omega(0, 0, 0.5) \simeq 0.1t_1$ corresponds to $\sim$10 meV] is also close to the experimental result. Here again, our results show that the 3D magnetism is well understood within the present itinerant spin picture [36,37].

Finally, let us discuss the relation between this 3D magnetism and SC. As we have seen, the SF in the nonhydrated systems becomes weak for small band fillings. This is because the nesting between the 2D outer and the 3D inner FS is not good. However, the nesting between the inner and the outer FS [38] can be restrengthened if the two-dimensionality is increased by hydration, resulting in enhanced SF. As we have mentioned in the beginning, our proposal is that this SF is responsible for SC [19]. Thus, in our view, the 3D magnetism and the incommensurate SF that gives rise to SC share the same origin as shown in Fig. 4: the nesting between the inner and the outer (connected or disconnected) FS that originate from the local minimum of the a_{1g} band.

Numerical calculations were performed at the facilities of the Supercomputer Center, ISSP, University of Tokyo. This study has been supported by Grants-in-Aid for Scientific Research from the Ministry of Education, Culture, Sports, Science and Technology of Japan and from the Japan Society for the Promotion of Science.

*Present address: NHK Spring, Yokohama, Japan.
†Present address: Nikon, Sagamihara, Japan.

[1] K. Takada *et al.*, Nature (London) **422**, 53 (2003).
[2] M. Z. Hasan *et al.*, Phys. Rev. Lett. **92**, 246402 (2004).
[3] H.-B. Yang *et al.*, Phys. Rev. Lett. **95**, 146401 (2005).
[4] T. Takeuchi *et al.*, in *Proceedings of the 24th International Conference on Thermoelectrics* (IEEE, Piscataway, NJ, 2005), p. 435.
[5] T. Shimojima *et al.*, Phys. Rev. Lett. **97**, 267003 (2006).
[6] D. J. Singh, Phys. Rev. B **61**, 13 397 (2000).
[7] K. Ishida *et al.*, J. Phys. Soc. Jpn. **72**, 3041 (2003).
[8] T. Fujimoto *et al.*, Phys. Rev. Lett. **92**, 047004 (2004).
[9] F. L. Ning *et al.*, Phys. Rev. Lett. **93**, 237201 (2004); F. L. Ning and T. Imai, Phys. Rev. Lett. **94**, 227004 (2005).
[10] Y. Ihara *et al.*, J. Phys. Soc. Jpn. **74**, 867 (2005).
[11] C. Michioka *et al.*, J. Phys. Soc. Jpn. **75**, 063701 (2006).
[12] Y. Ihara *et al.*, J. Phys. Soc. Jpn. **74**, 2177 (2005).
[13] I. R. Mukhamedshin *et al.*, Phys. Rev. Lett. **94**, 247602 (2005).
[14] Y. Kobayashi *et al.*, J. Phys. Soc. Jpn. **74**, 1800 (2005).
[15] G.-q. Zheng *et al.*, J. Phys. Condens. Matter **18**, L63 (2006).
[16] G.-q. Zheng *et al.*, Phys. Rev. B **73**, 180503 (2006).
[17] M. Yokoi *et al.*, J. Phys. Soc. Jpn. **73**, 1297 (2004).
[18] N. Oeschler *et al.*, cond-mat/0503690.
[19] K. Kuroki *et al.*, Phys. Rev. B **73**, 184503 (2006).
[20] M. Mochizuki and M. Ogata, J. Phys. Soc. Jpn. **75**, 113703 (2006); **76**, 013704 (2007); M. Mochizuki *et al.*, J. Phys. Soc. Jpn. **76**, 023702 (2007).
[21] T. Motohashi *et al.*, Phys. Rev. B **67**, 064406 (2003).
[22] J. Sugiyama *et al.*, Phys. Rev. B **67**, 214420 (2003); **69**, 214423 (2004).
[23] M. L. Foo *et al.*, Phys. Rev. Lett. **92**, 247001 (2004).
[24] S. P. Bayrakci *et al.*, Phys. Rev. B **69**, 100410 (2004).
[25] S. P. Bayrakci *et al.*, Phys. Rev. Lett. **94**, 157205 (2005).
[26] J. L. Gavilano *et al.*, Phys. Rev. Lett. **92**, 197201 (2004); L. M. Helme *et al.*, Phys. Rev. Lett. **94**, 157206 (2005).
[27] M. D. Johannes *et al.*, Phys. Rev. B **71**, 214410 (2005).
[28] J. L. Gavilano *et al.*, Phys. Rev. B **69**, 100404 (2004).
[29] Y. Wang *et al.*, Nature (London) **423**, 425 (2003).
[30] M. Daghofer *et al.*, Phys. Rev. Lett. **96**, 216404 (2006).
[31] Quite recently, M. M. Korshunov *et al.*, Pis'ma Zh. Eksp. Teor. Fiz. **84**, 769 (2006) [JETP Lett. **84**, 650 (2007)] discussed the relation between LMS and ferromagnetic SF but neglected the three-dimensionality of the system.
[32] N. E. Bickers, D. J. Scalapino, and S. R. White, Phys. Rev. Lett. **62**, 961 (1989).
[33] The terms ''inner'' and ''outer'' FS in the present study should not be mixed up with the commonly known ''bilayer-coupling-originated inner and outer'' a_{1g} FS, which in the unfolded BZ scheme correspond to FS at $k_z = 0$ and $k_z = \frac{\pi}{c/2}$ (see Fig. 2, $n = 1.60$).
[34] D. Qian *et al.*, Phys. Rev. Lett. **96**, 216405 (2006).
[35] We have investigated other sets of hopping values and found that the $(0, 0, \pi)$ spin correlation (with a possible slight incommensurability as expected from the nesting vector) is robust when the band filling is around $n \sim 1.8$ as far as LMS of the band exists.
[36] Y. V. Sushko *et al.* [J. Low Temp. Phys. **142**, 573 (2006)] find that the magnetic ordering temperature increases with applying pressure, unusual for an SDW state. In fact, applying pressure should increase $|t_z|/t_1$, which according to our FLEX calculation *favors* the SDW (as far as the increase of $|t_z|$ is within $\sim$10%) because the origin of the nesting here is the 3D FS itself. Applying pressure may also increase $|t_2|/t_1$ and $|t_3|/t_1$, which makes the LMS of the band deeper and, thus, also favors the SDW.
[37] Although it may not be so clear to what extent FLEX is reliable *quantitatively*, the conclusion that the 3D nesting results in a $(0, 0, \pi)$ SDW instability whose strength peaks around $n \sim 0.8$ can be naturally understood from the shape of the FS alone and should hold in any case. In other words, although vertex corrections are not considered in FLEX, such corrections at the level of, e.g., two-particle self-consistent approximation described by Y. M. Vilk and A.-M. S. Tremblay [J. Phys. I (France) **7**, 1309 (1997)], where the corrections are wave number independent, should not qualitatively affect the present result.
[38] The inner FS can appear despite the low Na content of $x \sim 0.35$ because of the presence of H_3O^+ ions suggested in, e.g., H. Sakurai *et al.*, Phys. Rev. B **74**, 092502 (2006).